APPLICATION OF PROBABILISTIC FRACTURE MECHANICS TO THE PTS ISSUE*

R. D. Cheverton D. G. Ball†

Oak Ridge National Laboratory
Oak Ridge, Tennessee 37831

ABSTRACT

As a part of the NRC effort to obtain a resolution to the PWR PTS issue a probabilistic approach has been applied that includes a probabilistic fracture-mechanics (PFM) analysis. The PFM analysis is performed with OCA-P, a computer code that performs thermal, stress and fracture-mechanics analyses and estimates the conditional probability of vessel failure, $P(F|E)$, using Monte Carlo techniques. The stress intensity factor (K_I) is calculated for two- and three-dimensional surface flaws using superposition techniques and influence coefficients. Importance-sampling techniques are used, as necessary, to limit to a reasonable value the number of vessels actually calculated.

Analyses of three PWR plants indicate that (1) the critical initial flaw depth is very small (5—15 mm), (2) the benefit of warm prestressing and the role of crack arrest are transient dependent, (3) crack arrest does not occur for the dominant transients, and (4) the single largest uncertainty in the overall probabilistic analysis is the number of surface flaws per vessel.

*Research sponsored by the Office of Nuclear Regulatory Research, U.S. Nuclear Regulatory Commission under Interagency Agreements 40-551-75 and 40-552-75 with the U.S. Department of Energy under Contract DE-AC05-840R21400 with Martin Marietta Energy Systems, Inc.

†Computing and Telecommunications Division, Martin Marietta Energy Systems, Inc.

DISCLAIMER

APPLICATION OF PROBABILISTIC FRACTURE MECHANICS TO THE PTS ISSUE*

R. D. Cheverton D. G. Ball

Oak Ridge National Laboratory
Oak Ridge, Tennessee 37831

1. INTRODUCTION

The pressurized-thermal-shock (PTS) issue is concerned with the possibility of failure of a pressurized-water-reactor (PWR) pressure vessel as a result of the combined effects of (1) pressure and thermal-shock loadings, (2) radiation damage to the vessel material, and (3) the existence of a sharp, crack-like defect (flaw) on the inner surface of the vessel. Thermal shock is a major contributor to the possibility of failure because it can result in relatively high tensile stresses and a reduction in fracture toughness near the inner surface, where the radiation-induced reduction in fracture toughness is the greatest; this combination of conditions introduces the possibility of initiation (incipient propagation) of very shallow inner-surface flaws.

The PTS issue has been under investigation for many years,[1-6] and the effort was accelerated when it was recognized that (1) the presence of copper (a tramp element) and nickel (an alloying element) enhance radiation damage, (2) existing PWR vessels may have "high" concentrations of these elements, and (3) a number of PWR PTS-type transients had already occurred. A preliminary generic analysis[7] of the Rancho Seco transient of 1978[8] indicated the possibility of vessel failure, given the necessary ingredients, long before normal end of plant life, and the Nuclear Regulatory Commission (NRC) declared PTS an unresolved safety issue (December 1981).

---

*Research sponsored by the Office of Nuclear Regulatory Research, U.S. Nuclear Regulatory Commission under Interagency Agreements 40-551-75 and 40-552-75 with the U.S. Department of Energy under Contract DE-AC05-84OR21400 with Martin Marietta Energy Systems, Inc.

Most of the early PTS analyses were of a conservative, deterministic nature; that is, a very severe PTS transient was assumed, high concentrations of copper and lower-bound fracture-toughness data were used, warm prestressing was ignored, and flaws of appropriate size were assumed to exist. Unfortunately, the results of such calculations indicated that very shallow flaws, which are difficult to detect, could lead to vessel failure before normal end of plant life.[7]

Even though the above analyses predicted premature failure, it was generally believed that because of the "conservative" nature of the analytical approach the probability of failure was actually very small. In an effort to obtain a better understanding of the nature and magnitude of the problem, the NRC proposed the development of a comprehensive probabilistic approach and established the Integrated Pressurized Thermal-Shock (IPTS) Program for this purpose (May 1981).

The IPTS effort included (1) the postulation of PTS transients for three specific PWR plants, (2) an estimation of their frequency of occurrence, (3) a systems analysis to determine the primary-system pressure, downcomer coolant temperature and fluid-film heat-transfer coefficient on the inner surface of the vessel, and (4) a probabilistic fracture-mechanics analysis that uses the information from item 3 as input. Item 4 provides an estimate of the conditional probability of vessel failure, $P(F|E)$, and this can be multiplied by the frequency of the corresponding transient, $\phi(E)$, and the product summed over all postulated transients to obtain the total frequency of failure, $\phi(F)$, for a specific plant; that is,

$$\phi(F) = \sum_n \phi_n(E) P_n(F|E) \quad , \qquad (1)$$

The individual products, $\phi_n(E)P_n(F|E)$ in Eq. (1) are of interest because they define the order of dominance; that is, they indicate the extent to which a transient contributes to $\phi(F)$ for a specific plant. The dominant transients might then be used in place of the "worst conceivable" for a less conservative deterministic fracture-mechanics analysis, if this "engineering" approach were preferred to the direct application of $\phi(F)$. In either case, it is necessary to calculate $P(F|E)$, and the development and application of a method for doing this in connection with the PTS issue is the primary subject of this paper.

2. PROBABILISTIC FRACTURE-MECHANICS MODEL

The probabilistic fracture-mechanics model developed for the IPTS program is included in the OCA-P[9] computer code, which accepts coolant-temperature, heat-transfer-coefficient and pressure transients as input and performs one-dimensional thermal and stress analyses for the vessel wall, fracture-mechanics analyses for two- and three-dimensional flaws, and a probabilistic analysis.

2.1 Fracture Mechanics Model

2.1.1 Stress intensity factor

The fracture-mechanics model in OCA-P is based on linear elastic fracture mechanics (LEFM), and this allows the stress intensity factor (K_I) to be calculated using superposition techniques in conjunction with influence coefficients, which are calculated with finite-element techniques.[10] The application of this procedure makes it possible to perform a large number of deterministic fracture-mechanics calculations at reasonable cost, a necessary condition for performing the probabilistic analysis. (Results of thermal-shock experiments conducted with large, thick-walled steel cylinders indicate that LEFM is applicable for the problem at hand.[11])

2.1.2 Fracture toughness

Material properties required for the fracture-mechanics analysis include the static crack initiation and arrest toughness values (K_{Ic} and K_{Ia}) and the nil-ductility reference temperature (RTNDT). For the probabilistic fracture-mechanics analysis, mean values of these parameters are required, and they were obtained for the vessel material as follows:

$$\overline{K}_{Ic} = 1.43 \left\{36.5 + 3.08 \exp\left[0.036(T - RTNDT + 56)\right]\right\}, \text{ MPa } \sqrt{m} , \quad (2)$$

$$\overline{K}_{Ia} = 1.25 \left\{29.5 + 1.34 \exp\left[0.026(T - RTNDT + 89)\right]\right\}, \text{ MPa } \sqrt{m} , \quad (3)$$

where the quantity in braces represents the ASME Section XI[12] lower-bound toughness value, and T is the temperature at the tip of the flaw in °C. These expressions were obtained by letting the ASME lower-bound curves represent the mean values minus two standard deviations (2σ) and by letting

$\sigma_{(K_{Ic})} = 0.15\ \overline{K}_{Ic}$ and $\sigma_{(K_{Ia})} = 0.10\ \overline{K}_{Ia}$.

In many cases, if crack arrest takes place, it must do so at or close to upper-shelf temperatures. Crack arrest under these conditions is not well understood but has been included in an approximate manner by specifying a maximum value of K_{Ia} that corresponds to the upper portion of an upper-shelf tearing resistance curve. As illustrated in Fig. 1, which is a plot of K_I vs crack depth (a/w, where a = crack depth, w = wall thickness) at a specific time in a PTS transient, if the load line (K_I vs a/w) intersects the K_{Ia} curve at $K_{Ia} < (K_{Ia})_{max}$, upper-shelf temperatures are not encountered. If, on the other hand, the load line misses the rising portion of the K_{Ia} curve and then decreases, as it does for some transients, there is, according to the model, a possibility of crack arrest at upper-shelf temperatures.

The tearing-resistance curve selected for the IPTS study represents a specific high-copper, low-upper-shelf, PWR-vessel weld material that had been

irradiated to a fluence of ~1.2 × 10^{19} neutrons/cm^2 at a temperature of ~290°C and tested at 200°C.[13] The upper, nearly flat portion of this curve corresponds to a K_J value of ~220 MPa $\sqrt{m}$, and this value was used for $(K_{Ia})_{max}$; K_J was obtained using the relation

$$K_J = \sqrt{JE} \ , \tag{4}$$

where

J = strain energy release rate,

E = Young's modulus.

The nil-ductility reference temperature (RTNDT) is equal to the sum of an initial value ($RTNDT_o$) and an increase due to radiation damage (ΔRTNDT); that is,

$$RTNDT = RTNDT_o + \Delta RTNDT \ . \tag{5}$$

The correlation used in the IPTS studies for the mean value of ΔRTNDT was essentially the same as that used in a preliminary NRC evaluation of PTS[14] and is

$$\overline{\Delta RTNDT} = 0.56 \ [-10 + 470 \ Cu + 350 \ Cu \ Ni] \ (F \times 10^{-19})^{0.27}, \ ^0C \tag{6}$$

or

$$\overline{\Delta RTNDT} = 0.56 \ [283 \ (F \times 10^{-19})^{0.194} - 48], \ ^0C \tag{7}$$

whichever is smaller, where

F = fast-neutron fluence (energy > 1 MeV), neutrons/cm^2,

Cu, Ni = concentrations of copper and nickel, wt %.

The attenuation of the fluence through the wall of the vessel was approximated with

$$F = F_o \ e^{-0.0094 \ a} \ , \tag{8}$$

where F_o is the fluence at the inner surface of the vessel and a is the crack depth in mm. The specific value of the coefficient in the exponent accounts to some extent for the effect of space-wise spectral changes on radiation damage.[14]

The fracture-toughness properties of the cladding material are very uncertain and are known to be dependent on the cladding-application process. The few experimental data that are available indicate that the radiation-induced reduction in fracture toughness can be similar to that for the base material.[15] As an expediency, which may or may not be conservative, it was assumed that for times of interest in the life of a vessel the cladding would have essentially the same fracture-toughness properties as the base material.

2.1.3 Warm prestressing

Fracture toughness is load- and temperature-history dependent, and some of the histories encountered in the IPTS studies result in fracture-toughness values greater than K_{Ic}. For instance, when $\dot{K}_I < 0$, a crack will not propagate,[11,16] and, if following a period of $\dot{K}_I < 0$ the stress intensity factor once again increases with time, the critical value of K_I may be substantially greater than K_{Ic}.[16] These phenomena are generally referred to as warm prestressing (WPS) and can have a significant effect on the potential for crack propagation during a PTS transient. OCA-P includes certain WPS features. However, because of uncertainties regarding details of load histories for postulated transients, there was reluctance to take advantage of WPS in the IPTS studies except for special cases where, following a loss of pressure, repressurization, and thus an increase in K_I, would not be possible (primary-system pipe breaks, valve failures, etc.).

2.1.4 Flaws

The region of the vessel of greatest concern with regard to PTS transients is that located between the ends of the core, where the fluence, and thus radiation damage, are substantially greater than elsewhere. Within this region, the vessels included in the IPTS studies are composed of sections of plate that are joined together with both axial and circumferential welds, as shown in Fig. 2. After the sections are joined, the inner surface of the composite cylinder is clad with ~5 mm of stainless steel.

The flaws of interest are surface cracks that extend through the cladding into the base material. Such flaws may be the result of the cladding process and thus could appear in plate sections as well as the welds that join the plates. In this regard, the plate region could contribute more to the probability of vessel failure than the welds because of the possibility of many more flaws in the plate. On the other hand, for many vessels the concentration of copper is substantially higher for the welds, while the concentration of nickel is about the same for the plates as for the welds. Thus, it is necessary to consider both the plate and weld regions, and these basic regions can be subdivided in accordance with possible variations in the combinations of F_o, $RTNDT_o$, Cu, Ni, and flaw density (N).

As indicated in Fig. 2, both two- and three-dimensional surface flaws are included in OCA-P and were considered for the IPTS studies. Because of a tendency for short and shallow flaws to extend on the surface to effectively become long, shallow flaws,[11,17] all initial flaws for the IPTS studies were assumed to be two dimensional. The surface length at arrest and for subsequent initiation-arrest events was specified as ~2 m (height of shell course) for axial flaws in high-copper axial welds, and was considered to be effectively infinite for all circumferential flaws and for axial flaws in plate regions (assuming low-copper plate).

The 2-m-length flaw was specified for deep axial flaws ($a/w > 0.2$) because an axial flaw in a high-copper axial weld is not likely to extend beyond the end of the weld into low-copper plate material (see Fig. 2), and because K_I values for a deep flaw of this length are substantially less than for a 2-D flaw.[18] An infinite length was selected for circumferential flaws because circumferential welds are continuous (Fig. 2), and the azimuthal variation in fluence generally is not large enough to justify otherwise. Offsetting this particular difference between circumferential and axial flaws, however, is a tendency for circumferential flaws to have lower values of K_I because of lower pressure stresses and a smaller deep-flaw bending effect.[11] Propagation of all flaws was judged on the basis of the K ratios (K_I/K_{Ic}, K_I/K_{Ia}) at the deepest point of the flaw.

2.1.5 Cladding

OCA-P treats cladding on the inner surface of the vessel as a discrete region to the extent that thermal and stress effects are included. The effect of cladding on the surface extension of a flaw is not known and thus not included.

2.2 Probabilistic Model

2.2.1 Basic concept

The OCA-P probabilistic model, which is similar to that developed by Gamble and Strosnider,[19] is based on Monte Carlo techniques; that is, a large number of vessels is simulated, and each vessel is then subjected to a fracture-mechanics analysis to determine whether the vessel will fail. Each vessel is defined by randomly selected values of several parameters that are judged to have significant uncertainties associated with them. The calculated probability of vessel failure is simply the number of vessels that fail

divided by the total number of vessels generated. It constitutes a conditional probability of failure, $P(F|E)$, because the assumption is made that the PTS transient (event) takes place. A logic diagram summarizing the various steps in the OCA-P probabilistic analysis is shown in Fig. 3.

2.2.2 Parameters simulated

Parameters simulated for the IPTS studies were crack depth (a), fast neutron fluence (F), concentrations of copper (Cu) and nickel (Ni), crack-initiation toughness (K_{Ic}), crack-arrest toughness (K_{Ia}), $RTNDT_o$ and $\Delta RTNDT$. Normal distributions were assumed for each of these parameters except the crack depth; standard deviations and truncation values used in the analysis are included in Table 1.

As a convenience, but at the expense of introducing some additional uncertainty in the estimation of $\phi(F)$, $RTNDT_s$ (the value of RTNDT at the inner surface) can be used as an independent variable in lieu of F_o, Cu, Ni and $RTNDT_o$. To do this, Eq. (7) is ignored, and Eq. (6) is combined with Eq. (8) to obtain

$$\Delta RTNDT(a) = \Delta RTNDT_s \, e^{-0.0025\, a} , \qquad (9)$$

where $\Delta RTNDT(a)$ is the value of $\Delta RTNDT$ at the tip of the flaw. Assuming a nominal value of $RTNDT_o$ and combining Eq. (9) with Eq. (5) allows one to use Eqs. (2) and (3) directly without having to specify F_o, Cu and Ni.

When using $RTNDT_s$ as an independent variable, an appropriate distribution function must be developed. For the IPTS studies this was done by performing a Monte Carlo analysis with Eq. (6), in which case F_o and Cu were simulated, and different values of $\overline{F_o}$, $\overline{Cu}$ and $\overline{Ni}$ were included. Based on this analysis, a normal distribution with $1\sigma = 0.14\ \overline{\Delta RTNDT}$ was selected for $\Delta RTNDT_s$. The additional uncertainty mentioned above is the result of the distribution and

thus P(F|E) being a function of $\overline{F_o}$, $\overline{Cu}$ and $\overline{Ni}$, particularly $\overline{Cu}$. Furthermore, for a given value of RTNDT, P(F|E) is somewhat sensitive to the value of $RTNDT_o$. The standard deviation selected for ΔRTNDT was based on $\overline{Cu}$ = 0.25 wt %, and when $RTNDT_s$ was used as an independent variable, −18°C was selected for $RTNDT_o$.

2.2.3 Flaw density

The number of flaws in a specific region with a depth in a specific range of crack depths Δa_i is given by

$$N_j(\Delta a_i) = N_j A_j \int_{\Delta a_i} f(a)B(a)da \,, \tag{10}$$

where

N_j = number of flaws of all depths per unit surface area of ~~a specific~~ the jth region,

A_j = surface area of the ~~specific~~ jth region,

$f(a)$ = flaw-depth density function,

$B(a)$ = probability of nondetection.

The parameters N_j and $f(a)$ pertain to vessel conditions prior to preservice inspection and repair, and $B(a)$ is derived on the basis of repairing or otherwise disposing of all detected flaws.

The value of N_j and the functions $f(a)$ and $B(a)$ are not well known because most of the available inspection data do not pertain to surface flaws that extend into and through the cladding of a PWR pressure vessel. For the IPTS studies the functions $f(a)$ and $B(a)$ were those suggested in the Marshall Report[20] and are as follows:

$$f(a) = 0.16\, e^{-0.16\, a},\ mm^{-1}, \tag{11}$$

$$B(a) = 0.005 + 0.995\, e^{-0.113\, a}\,, \tag{12}$$

where

a = crack depth, mm ,

$$\int_0^W f(a)da = 1 \ .$$

2.2.4 Conditional probability of vessel failure

The calculated probability of vessel failure must include the contributions from all regions of the vessel. For $P_j(F|E) < 0.1$,

$$P(F|E) \approx \sum_j P_j(F|E) \ . \tag{13}$$

The total number of flaws per region is

$$n_j = N_j A_j \int_0^W f(a)B(a)da \ , \tag{14}$$

and when $n_j \leq 1$,

$$P_j(F|E) = \hat{P}_j \, n_j \ , \tag{15}$$

where $\hat{P}_j = \frac{N'_{fj}}{N'_{vj}}$,

N'_{fj} = number of vessels, with a flaw in the jth region, that fail,

N'_{vj} = number of vessels simulated with a flaw in the jth region.

When $n_j > 1$,

$$P_j(F|E) = n_j \hat{P}_j - \frac{n_j(n_j - 1)}{2!} \hat{P}_j^2 + \frac{N_j(n_j - 1)(n_j - 2)}{3!} \hat{P}_j^3 - \ldots \tag{16}$$

$$+ (-1)^{n_j - 1} \hat{P}_j^{n_j}$$

It is apparent that Eq. (15) is also appropriate with $n_j > 1$, provided that $\hat{P}_j \ll 1$.

2.2.5 Importance sampling

For very small values of $P(F|E)$, the values of N'_{vj} required to achieve reasonable accuracy becomes quite large. Under some circumstances the value of N'_{vj} can be reduced by using importance sampling techniques.[21] For the IPTS studies this was done by eliminating flaw depths that did not contribute significantly to initiation and by sampling only the tails of the distribution functions for other simulated parameters. The portion of the distribution function not sampled is accounted for by multiplying the number of simulated vessels, N'_{vj}, by a correction factor. Equation (15) then becomes

$$P(F|E) = \sum_j \frac{\hat{P}_j}{\prod_k F_{kj}} N_j A_j \int_o^w f(a)B(a)da \ , \qquad (17)$$

where

F_{kj} = correction factor for kth simulated parameter.

Values of F_k are a function of the points on the distribution curve at which sampling is started and stopped (truncation point). For the IPTS studies, when importance sampling was used for the flaw-depth density function, only the first flaw-depth increment was omitted. Thus,

$$F_k \text{ (flaw depth density)} = \frac{1}{\int_{\Delta a_1}^{w} f(a)B(a)da} = 3.24 \ .$$

Table 2 includes values of F_k for several different starting points on a normal distribution curve that is truncated at 3σ.

For the IPTS studies, importance sampling was applied to three simulated parameters, including flaw depth, and for many cases the starting point on the

normal distribution curves was 1.25σ. Thus, $\prod_k F_k = 300$, which represents a significant savings in computer costs for the same accuracy in P(F|E)).

2.2.6 Statistical error

The minimum number of simulated vessels required to satisfy a specified accuracy is estimated by applying the central limit theorem.[21] Using this approach, and specifying a 95% confidence level yields

$$\hat{P}_j(F|E) = \frac{\hat{P}_j N_j A_j}{\prod_k F_{kj}} \int_o^w f(a)B(a)da \pm 1.96\,\sigma_j \,, \tag{18}$$

where

$$\sigma_j = \frac{1}{\prod_k F_{kj}} \left[\frac{\hat{P}_j(1-\hat{P}_j)}{N'_{vj}} \right]^{1/2} \cdot N_j A_j \int_o^w f(a)B(a)da \,. \tag{19}$$

The values of σ corresponding to all of the vessels simulated is

$$\sigma_{P(F|E)} = \sqrt{\Sigma \sigma_j^2} \,, \tag{20}$$

and the error, ε_j, associated with the jth region is

$$\varepsilon_j = \frac{1.96\,\sigma_j \prod_K F_{kj}}{\hat{P}_j N_j A_j \int_o^w f(a)B(a)da} \,. \tag{21}$$

For $\hat{P}_j \ll 1$,

$$\varepsilon_j \approx 1.96 \left(\frac{1}{\hat{P}_j N'_{vj}} \right)^{1/2} = 1.96 \left(\frac{1}{N'_{fj}} \right)^{1/2} \,. \tag{22}$$

The total error, ε, considering all regions of interest is

$$\varepsilon = \frac{\pm 1.96\,\sigma_{P(F|E)}}{\sum_j \frac{\hat{P}_j\, NV_j}{\prod_k F_{kj}} \int_0^w f(a)B(a)da} \qquad (23)$$

It is of interest to note (Eq. 22) that the error for a single region, ε_j, is only a function of N'_{fj}. According to Refs. 22 and 23, for the estimate of ε_j to be "reasonably" accurate, N'_{fj} should be greater than 5 (Ref. 22) or perhaps 9 (Ref. 23).

2.2.7 Failure criteria

After an appropriate number of vessels has been simulated, each vessel is subjected to a fracture-mechanics analysis to determine if failure will occur during a particular transient at a specific time in the life of the plant. For the IPTS studies, failure was assumed to occur if, following an initiation event ($K_I = K_{Ic}$ at deepest point of flaw), K_I remained greater than K_{Ia} up to or beyond the point at which plastic instability occurred in the remaining ligament (Fig. 1). Thus, failure was defined as through-wall cracking, which does not necessarily imply an inability of the vessel to retain sufficient coolant to cover the core. The consequences of through-wall cracking are evaluated in a separate study.[24]

3. PLANTS INCLUDED IN IPTS STUDIES

Three nuclear plants (Oconee-1, Calvert Cliffs-1 and H. B. Robinson-2), each one representing a different nuclear vendor and utility, were selected for the IPTS studies. In addition, one hypothetical reactor vessel (HBR-HYPO) was included for the purpose of more appropriately illustrating the probabilistic fracture-mechanics methods of analysis. Information pertaining to these plants and their reactor vessels is provided in Table 3, and a typical set of pressure and temperature transients for a rather severe transient is shown in Fig. 4.

4. TRENDS DEDUCED FROM IPTS STUDIES

It is not the intent of this paper to discuss in detail the results of the IPTS studies (preliminary results are included in Refs. 25-27). However, some of the fracture-mechanics-oriented trends should be mentioned.

4.1 P(F|E) vs Effective Full-Power Years (EFPY)

Because of the accumulative effect of radiation damage [Eqs. (6) and (7)], P(F|E) increases with reactor operating time and thus with RTNDT, as indicated in Fig. 5 for the transient in Fig. 4. It is of interest to note that for this particular transient increasing RTNDT from 40 to 100°C increases P(F|E) by a factor of more than 10^4.

4.2 Relative Contribution of Plate and Weld

As indicated in Table 3, for Oconee-1, Calvert Cliffs-1, and HBR-HYPO, RTNDT for the plate region is much less than for the dominant axial weld, but the area of the plate is much greater than for the welds. The net effect, assuming the same flaw density (N_j) for all regions, is that the axial weld included in Table 3 is the dominant contributor to P(F|E). For HBR-2 the plate region has the largest value of RTNDT as well as area and thus is the dominant contributor to P(F|E).

4.3 The Role of Crack Arrest

Crack arrest can take place and prevent failure of the vessel, if the primary-system pressure is low enough, in which case the value of $(K_{Ia})_{max}$ influences P(F|E).[27] However, for high-pressure transients, such as that illustrated in Fig. 4, crack arrest does not take place, irrespective of the value of $(K_{Ia})_{max}$, because K_I is more sensitive to crack depth than K_{Ia} is. Thus,

the role of crack arrest is dependent on which transients are dominant, that is, which ones contribute the most to $\phi(F)$. For the IPTS studies the dominant transients were high-pressure transients. Therefore, the value of $(K_{Ia})_{max}$ used in the studies was not critical.

4.4 Time of Events, Duration of Transient and Warm Prestressing ($\dot{K}_I < 0$)

The time in the transient at which most events take place is transient dependent, and the effects of WPS and of the duration of the transient are dependent on the time of the events. This is illustrated in Fig. 6, which is a histogram of percent failures vs time of failures for two Oconee-1 dominant transients (O-A and O-B), indicating the time for each transient at which $\dot{K}_I = 0$ (incipient warm prestressing). For both transients the time of incipient WPS is early in the transient (20–30 min), and $\dot{K}_I$ is less than zero for the remainder of the 2-h transients. Ignoring warm prestressing, failure for one transient (O-B) occurs much later, in which case the inclusion of WPS would eliminate all indicated failures. For the other transient (O-A), about one half of the failures occurred before incipient WPS.

The factors by which $P(F|E)$, for the five most dominant transients, and $\phi(F)$ are reduced by the inclusion of WPS are indicated in Table 4. It is apparent that although the benefit may be large for some individual transients, it may not be very large for $\phi(F)$, depending on which transients are dominant.

4.5 Critical Flaw Depths

Most of the initial flaws that resulted in failure were very shallow (5–15 mm), and most of these resided entirely within the cladding. Such flaws are difficult to detect, and thus essentially no data regarding flaw surface

density are available. As a result, the uncertainty in N_j and thus $P(F|E)$ and $\phi(F)$ is quite large. As a part of the IPTS studies, the uncertainty factor for $\phi(F)$ was estimated to be $\sim 10^3$, and the single largest contributor to this uncertainty was N_j.

5. DISCUSSION AND ~~SUMMARY~~ conclusions

A probabilistic fracture-mechanics model was developed as a part of the NRC Integrated Pressurized Thermal-Shock Program to help resolve the PWR pressurized-thermal-shock issue. The model is based on linear elastic fracture mechanics and considers both two- and three-dimensional flaws. Monte Carlo techniques are used to calculate the conditional probability of vessel failure, and importance sampling is used to reduce the number of vessels that must be simulated.

The flaws of concern are those that extend from the inner surface into and through the cladding, and it was found that very shallow (5—15 mm) flaws were responsible for most of the calculated failures. Because essentially no inspection data are available for such flaws, the number of these flaws per vessel is the single largest uncertainty in the analysis.

The cladding is included in the thermal and stress analyses, but because of a lack of radiation-damage data, it is assumed that the cladding will not prevent surface extension of the initially short and shallow flaws. If surface extension is impeded by the cladding, the calculated probability of failure will be much less. (The actual effects of cladding are under investigation.[15,29])

The benefit of warm prestressing ($\dot{K}_I < 0$) was investigated and was found to be dependent on the transient. Thus, the effect on the overall frequency of failure is dependent on which transients are dominant. For one of the

nuclear plants considered, the inclusion of warm prestressing reduced the frequency of failure by only a factor of 5. For another the factor was ~100. (WPS effects with $\dot{K}_I > 0$ are under investigation.[30])

Crack arrest will prevent vessel failure for low-pressure but not high-pressure transients. These latter transients are the dominant contributors to the frequency of failure. Thus, to reduce the frequency of failure it is necessary to prevent propagation of the initial shallow flaws. (Crack-arrest behavior at elevated temperatures is also being investigated.[30])

References

1. W. H. Tuppeny, Jr., W. F. Siddall, Jr., and L. C. Hsu, *Thermal Shock Analysis on Reactor Vessels Due to Emergency Core Cooling System Operation*, Combustion Engineering, Inc., Docket 50309, NTIS, 1968.

2. R. C. Hutto, C. D. Morgan, and W. A. Van Der Sluys, *Analysis of the Structural Integrity of a Reactor Vessel Subjected to Thermal Shock*, Report BAW-10018, Babcock & Wilcox Company, May 1969.

3. D. J. Ayres and W. F. Siddall, *Finite Element Analysis of Structural Integrity of a Reactor Pressure Vessel During Emergency Core Cooling*, Report A-70-10-2, Combustion Engineering, Inc., January 1970.

4. C. A. Buchalet and W. H. Bamford, "Methods of Fracture Mechanics Analysis of Nuclear Reactor Vessels Under Severe Thermal Transients," ASME Paper 75-WA/PVR-3, 1975.

5. R. D. Cheverton, "Thermal-Shock Studies Associated with Injection of Emergency Core Coolant Following A Loss-of-Coolant Accident in PWRs, *Nuclear Safety*, Vol. 19, No. 1, January February 1978.

6. R. D. Cheverton, S. K. Iskander, and G. D. Whitman, "The Integrity of PWR Pressure Vessels During Overcooling Accidents," *Proceedings of the International Meeting on Thermal Nuclear Reactor Safety*, NUREG/CP-0027, Vol. 1, Feb. 1983, pp. 421–430.

7. R. D. Cheverton, Parametric Analysis of Rancho Seco Overcooling Accident, letter to M. Vagins (USNRC), March 1981, available at NRC Public Document Room.

8. Memorandum from Scaramento Municipal Utility District to Nuclear Regulatory Commission Director of Regulatory Operations, Region IV, Subject: "Reactor Cooldown Rate Exceeds Limit Following Trip at Rancho Seco," NSIC Accession 00ZO-138830, available at NRC Public Document Room, Mar. 31, 1978.

9. R. D. Cheverton and D. G. Ball, *OCA-P, A Deterministic and Probabilistic Fracture-Mechanics Code for Application to Pressure Vessels*, NUREG/CR-3618 (ORNL-5991), Union Carbide Corp., Nuclear Div., Oak Ridge Natl. Lab., (May 1984).

10. D. G. Ball, B. R. Bass, J. W. Bryson, R. D. Cheverton and J. B. Drake, *Stress-Intensity-Factor Influence Coefficients for Surface Flaws in Pressure Vessels*, NUREG/CR-3723 (ORNL/CSD/TM-216), Martin Marietta Energy Systems, Inc., Oak Ridge Natl. Lab., February 1985.

11. R. D. Cheverton et al., *Pressure Vessel Fracture Studies Pertaining to the PWR Thermal-Shock Issue: Experments TSE-5, TSE-5A and TSE-6*, NUREG/CR-4249 (ORNL-6163), June 1985.

12. T. U. Marston (Ed.), *Flaw Evaluation Procedures, ASME Section XI, Background and Application of ASME Section XI, Appendix A, Special Report*, EPRI NP-719-SR, American Society of Mechanical Engineers, Electric Power Research Institute, August 1978.

13. Letter from F. J. Loss (NRL) to R. [illegible] Bryan (ORNL), March 31, 1981.

14. NRC Staff Evaluation of Pressurized Thermal Shock, Sept. 13, 1982 draft, attachment to transmittal document Secy 82-465, Nov. 23, 1982 (available in NRC Public Document Room).

15. W. R. Corwin, *Assessment of Radiation Effects Relating to Reactor Pressure Vessel Cladding*, NUREG/CR-3671 (ORNL-6047), July 1984.

16. F. J. Loss, R. A. Gray, Jr., and J. R. Hawthorne, *Significance of Warm Prestress to Crack Initiation During Thermal Shock*, Report NRL/NUREG-8165, Naval Research Laboratory, NTIS, Sept. 29, 1977.

17. R. D. Cheverton et al., *Pressure Vessel Fracture Studies Pertaining to the PWR Thermal-Shock Issue: Experiment TSE-7*, NUREG/CR-XXXX (ORNL-6177), (in preparation).

18. R. D. Cheverton and D. G. Ball, "A Reassessment of PWR Pressure Vessel Integrity During Overcooling Accidents, Considering 3-D Flaws," *Journal of Pressure Vessel Technology*, November 1984, Vol 106 (375—382).

19. R. M. Gamble and J. Strosnider, Jr., *An Assessment of the Failure Rate for the Beltline Region of PWR Pressure Vessels During Normal Operation and Certain Transient Conditions*, NUREG/0778, June 1981.

20. W. Marshall, *An Assessment of the Integrity of PWR Pressure Vessels*, United Kingdom Atomic Energy Authority, Second Report, March 1982.

21. R. Y. Rubinstein, *Simulation and the Monte Carlo Method*, Israel Institute of Technology, John Wiley & Sons, New York, 1981, pp. 115-117.

22. P. G. Hoel, *Introduction to Mathematical Statistics*, 3rd Addition, 1962, John Wiley & Sons.

23. A. Hald, *Statistical Theory with Engineering Applications*, John Wiley & Sons, 1952.

24. F. A. Simonen et al., *States of Vessel Failure Mode Analysis: Feasibility Study and Preliminary Evaluation*, Dec. 1983 draft, Pacific Northwest Laboratory.

25. T. J. Burns et al., *Pressurized Thermal-Shock Evaluation of the Oconee-1 Nuclear Power Plant*, NUREG/CR-3770 (ORNL/TM-9176), April 13, 1984 (Draft).

26. D. L. Selby et al., *Pressurized Thermal-Shock Evaluation of the Calvert Cliffs Unit 1 Nuclear Power Plant*, NUREG/CR-4022 (ORNL/TM-9408), Oct. 9, 1984 (Draft).

27. D. L. Selby et al., *Pressurized Thermal Shock Evaluation of the H. B. Robinson Unit 2 Nuclear Power Plant*, NUREG/CR-4183 (ORNL/TM-9567), March 1985 draft.

28. R. D. Cheverton and D. G. Ball, "The Role of Crack Arrest in the Evaluation of PWR Pressure Vessel Integrity During the PTS Transients," to be published in *Engineering Fracture Mechanics*.

29. W. R. Corwin, G. C. Robinson, R. K. Nanstad, J. G. Merkle, R. G. Berggren, G. M. Goodwin, R. L. Swain, and T. D. Owings, *Effects of Stainless Steel Weld Overlay Cladding on the Structural Integrity of Flawed Steel Plates in Bending, Series 1*, NUREG/CR-4015 (ORNL/TM-9390), Oak Ridge Natl. Lab., Oak Ridge, Tennessee (April 1985).

30. R. H. Bryan, B. R. Bass, S. E. Bolt, J. W. Bryson, D. P. Edmonds, R. W. McCulloch, J. G. Merkle, R. K. Nanstad, G. C. Robinson, K. R. Thoms and G. D. Whitman, *Pressurized-Thermal-Shock Test of 6-in.-Thick Pressure Vessels. PTSE-1: Investigation of Warm Prestressing and Upper-Shelf Arrest*, NUREG/CR-4106 (ORNL-6135), Oak Ridge National Laboratory, Oak Ridge, Tenn. (April 1985).

Table 1. Parameters simulated in OCA-P

Parameter	Standard[a] deviation (σ)	Truncation
Fluence (F)	0.3 μ(F)	F = 0
Copper	0.025%	+0.40
Nickel	0.0	-
$RTNDT_o$	9°C[b]	*b*
$\Delta RTNDT^c$	13°C[b,c]	*b*
$\Delta RTNDT^d$	0.14 $\mu(\Delta RTNDT)^d$	$\pm 3\sigma$
K_{Ic}	0.15 $\mu(K_{Ic})$	$\pm 3\sigma$
K_{Ia}	0.10 $\mu(K_{Ia})$	$\pm 3\sigma$

[a] Normal distribution used for each parameter.

[b] $\sigma_{(RTNDT)} = \left[\sigma^2(RTNDT_o) + \sigma^2(\Delta RTNDT)\right]^{1/2}$, truncated at $\pm 3\sigma$.

[c] Accounts for uncertainty in correlation.

[d] Accounts for uncertainty in Cu, Ni and F_o when $RTNDT_s$ used as independent variable.

Table 2. Values of F_k for a normal distribution truncated at 3σ

Start of sampling (No. of standard deviations above mean)	Fraction of distribution not simulated	r_k
1.0	0.8422	6.3
1.25	0.8954	9.6
1.50	0.9343	15.2
1.75	0.9611	25.7
2.00	0.9784	46.4
2.25	0.9891	91.7
2.60	0.9951	204.1
2.75	0.9983	588.2

Table 3. Information pertaining to nuclear plants included in IPTS studies

Plant Designer Utility	Region	Chemistry, wt% Ni	Cu	RTNDT$_o$ °C	F_c^b 10^{19} n/cm^2	Area m^2	$\overline{RTNDT}^c$ °C
Oconee-1	Axial weld[a]	0.29	0.55	−7	1.1	0.2	97
B&W	Cir. weld[a]	0.26	0.61	−7	0.9	1.0	84
Duke Power	Plate	0.12	0.60	4	1.2	50	46
Calvert Cliffs-1	Axial weld[a]	0.21	0.87	−49	6.1	0.12	90
CE	Cir. weld[a]	0.24	0.18	−62	6.1	0.64	46
BG&E	Plate	0.12	0.64	−12	6.1	50	55
H. B. Robinson-2	Axial weld[a]	0.22	0.04	−49	3.2	0.14	24
Westinghouse	Cir. weld[a]	0.19	0.80	−49	2.0	0.46	39
CP&L	Plate	0.12	0.10	8	4.2	50	49
HBR-HYPO	Axial weld[a]	0.22	0.80	−18	3.2	0.14	99
	Cir. weld[a]	0.22	0.80	−18	2.0	0.46	85
	Plate	0.12	0.80	−18	4.2	50	48

[a]Dominant weld region only.

[b]Inner-surface fluence at 32 EFPY (maximum in region).

[c]Inner-surface value of $\overline{RTNDT}$ at 32 EFPY.

Table 4. Benefit of warm prestressing for Oconee-1, Calvert Cliffs-1 and HBR-HYPO

Transient (in order of dominance)	Plant		
	Oconee-1	Calvert Cliffs-1	HBR-HYPO
	$P(F\|E)_{WPS}/P(F\|E)$		
1	$<10^{-3}$	$<2 \times 10^{-3}$	9×10^{-3}
2	3×10^{-1}	1	$<2 \times 10^{-3}$
3	$<10^{-3}$	$<1 \times 10^{-2}$	$<2 \times 10^{-3}$
4	$<10^{-3}$	1×10^{-1}	$<2 \times 10^{-3}$
5	3×10^{-1}	$<5 \times 10^{-1}$	5×10^{-2}
	$\Phi(F)_{WPS}/\Phi(F)$		
	1×10^{-1}	2×10^{-1}	7×10^{-3}

DETERMINISTIC ANALYSIS COMPARES K_I WITH K_{Ic} AND K_{Ia} TO FIND EARLIEST TIME OF FAILURE FOR EACH SIMULATED VESSEL

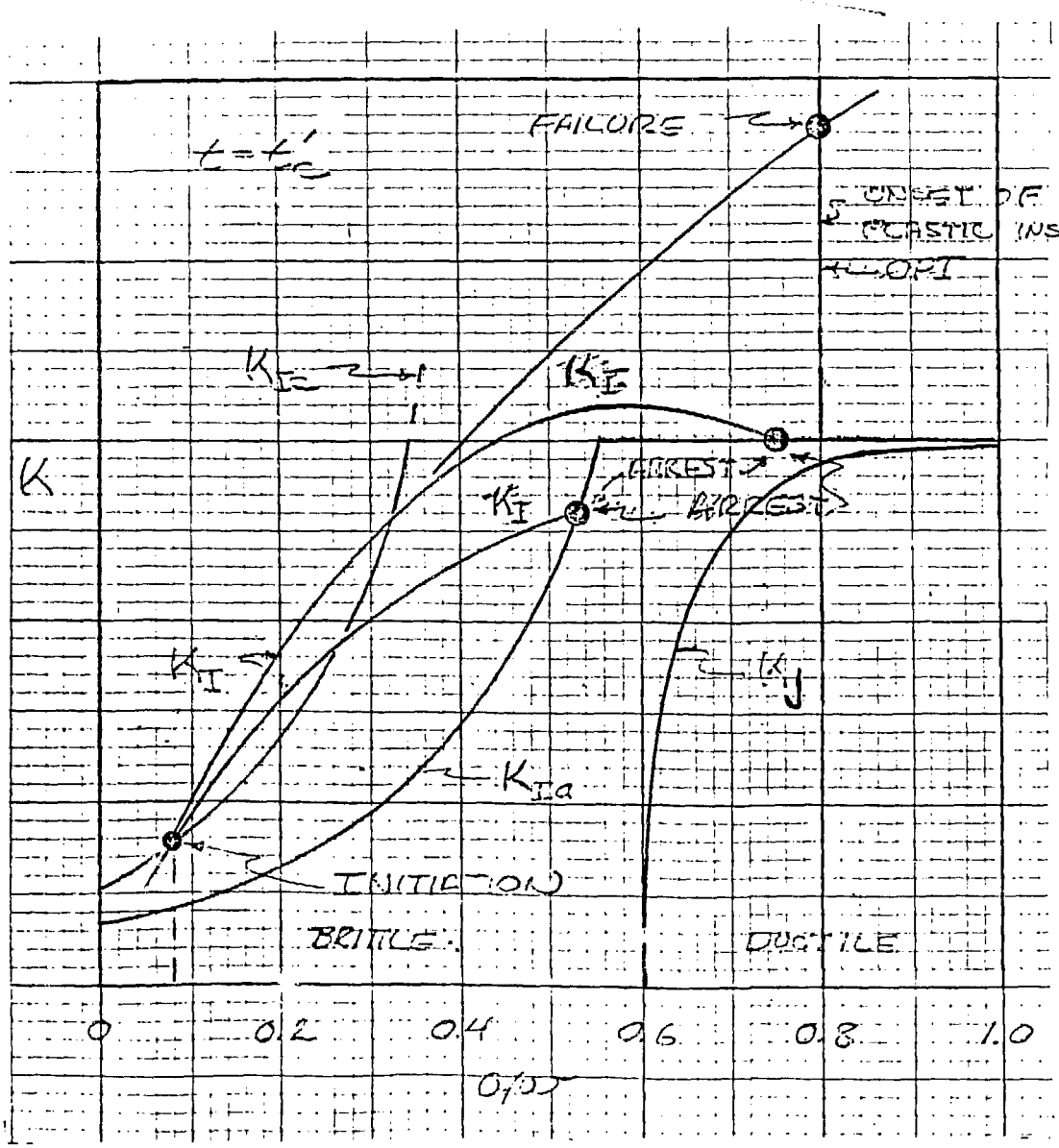

FIG 1 Illustration of arrest, failure, and method for selecting $(K_{Ia})_{max}$

ORNL–DWG 84–6260 ETD

TWO FLAW GEOMETRIES (2–D, 3–D) AND THREE FLAW REGIONS (PLATE, AXIAL AND CIRCUMFERENTIAL WELDS) CONSIDERED

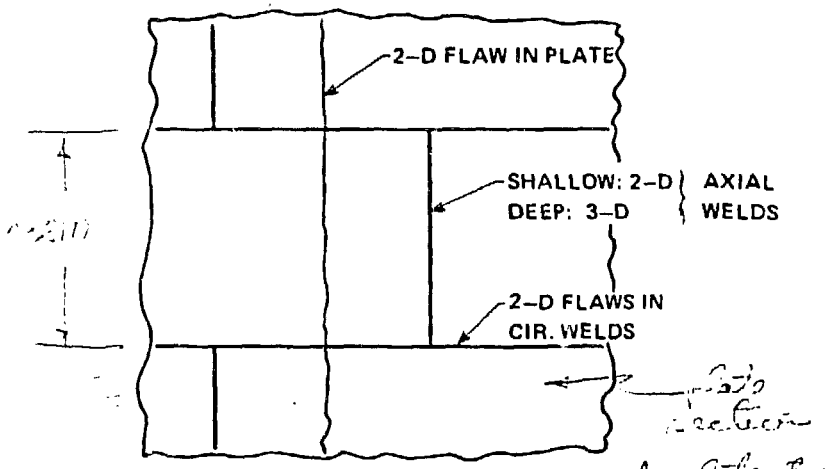

DEVELOPED VIEW OF BELTLINE REGION

ORNL WS–35617 ETD

LARGE–SCALE THERMAL–SHOCK AND PRESSURIZED–THERMAL–SHOCK EXPERIMENTS CONDUCTED TO VERIFY FM METHODS OF ANALYSIS

- LEFM VALID
- CRACK–ARREST CONCEPT VALID
- WARM PRESTRESSING DEMONSTRATED
- CLADDING RESTRAINT
- ARREST ON UPPER SHELF

} UNDER INVESTIGATION

ORNL - DWG 84 -4174A ETD

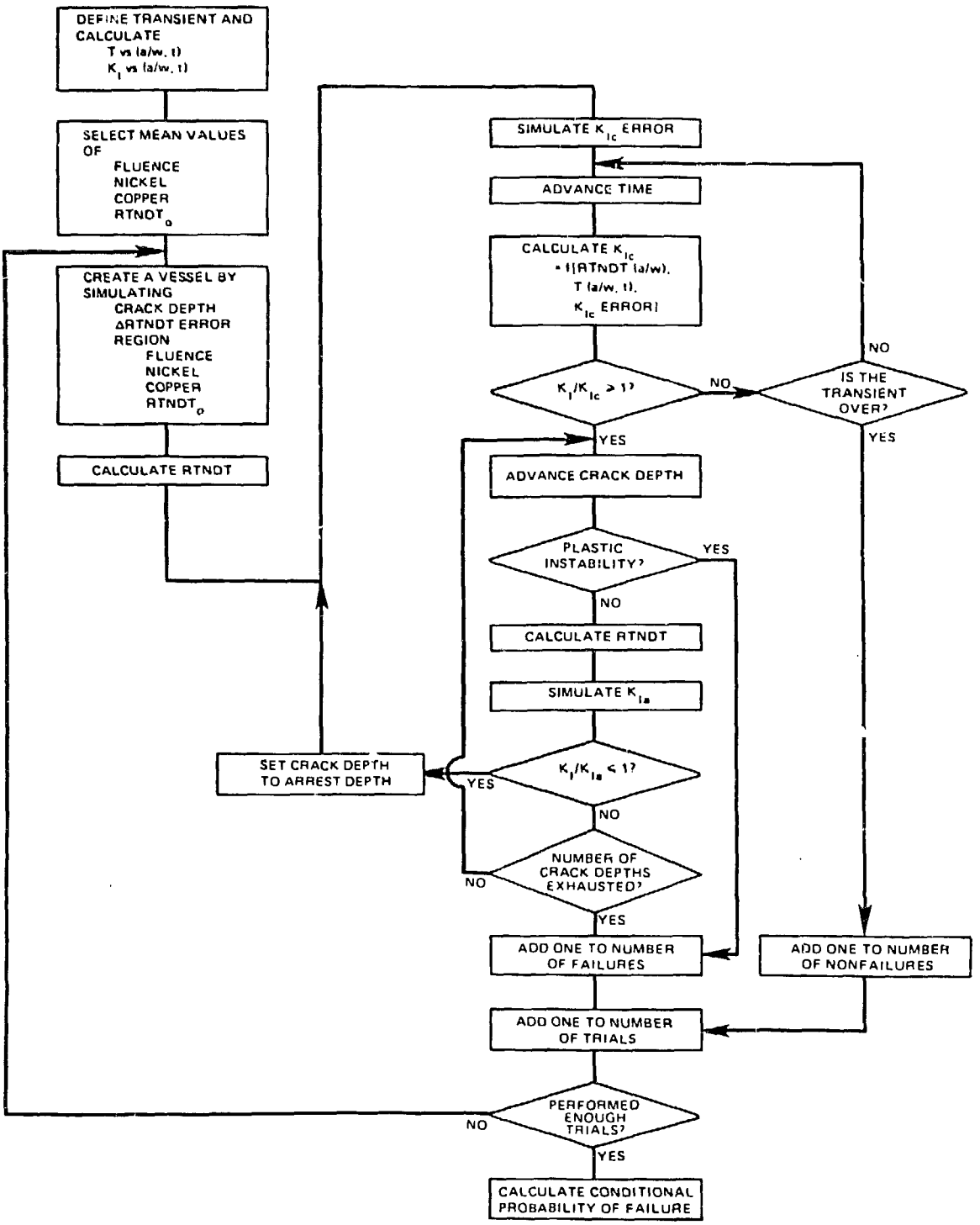

same as for paper

DRAFT

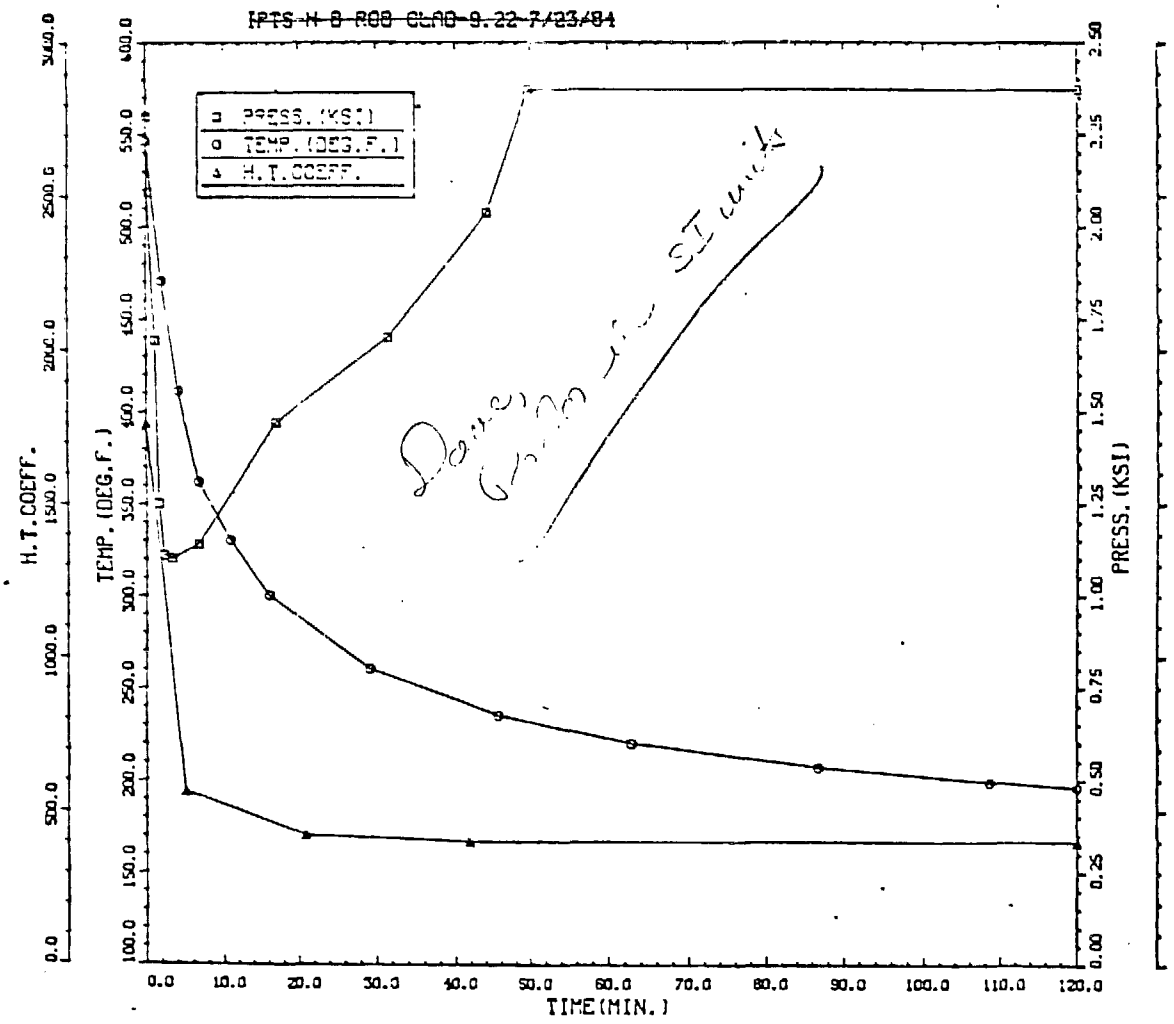

4 and vs time

Figure 5.13. Downcomer coolant temperature, primary-system pressure, and fluid-film-heat-transfer coefficient vs time (~~Transient 9.22~~B).

for a typical severe PTS transient

5/31/83

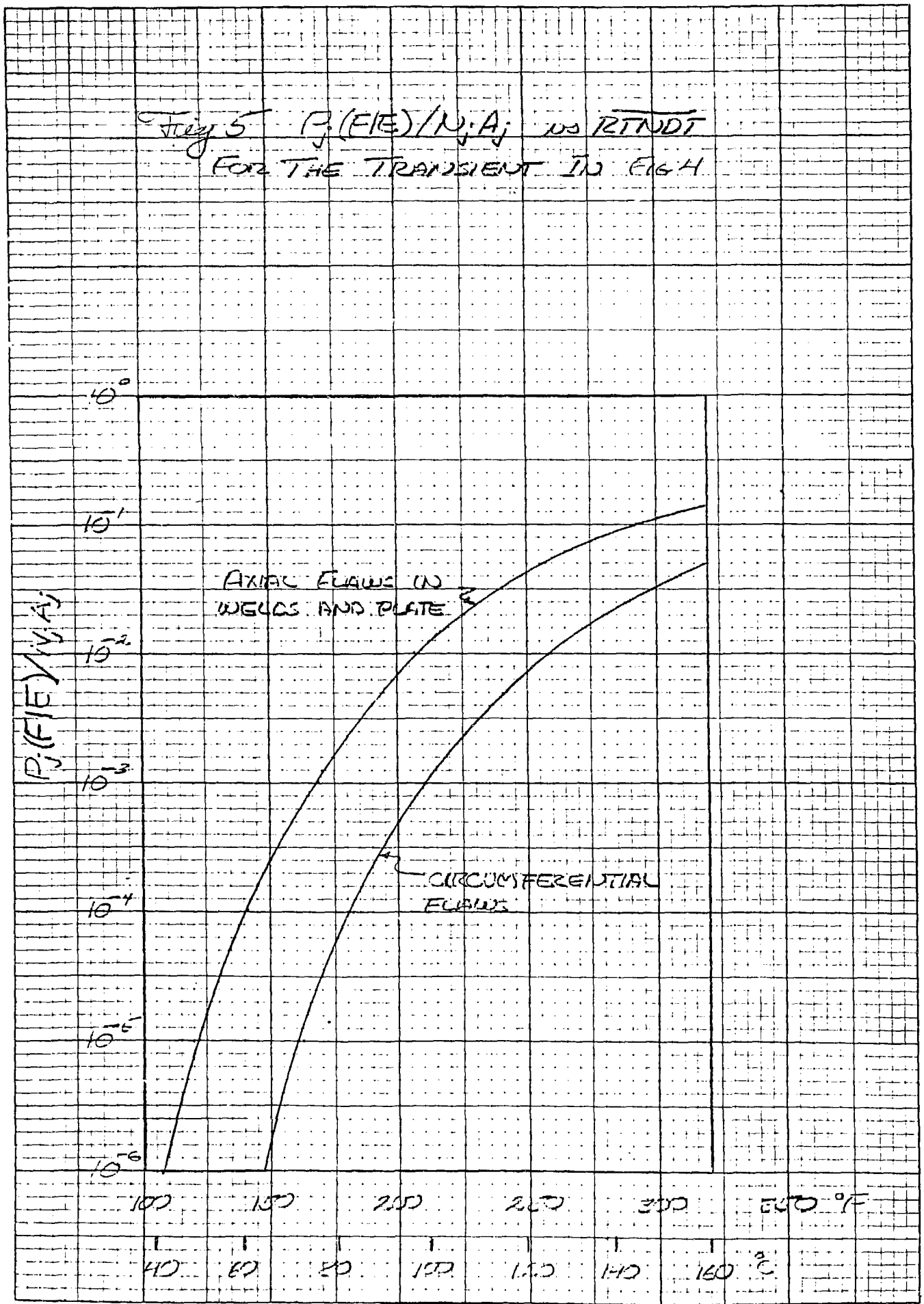

ORNL-DWG 84-6200 ETD

~~RESULTS INDICATE BENEFIT OF SHORTER DURATION, INCLUSION OF WPS~~

~~BENEFIT TRANSIENT DEPENDENT~~

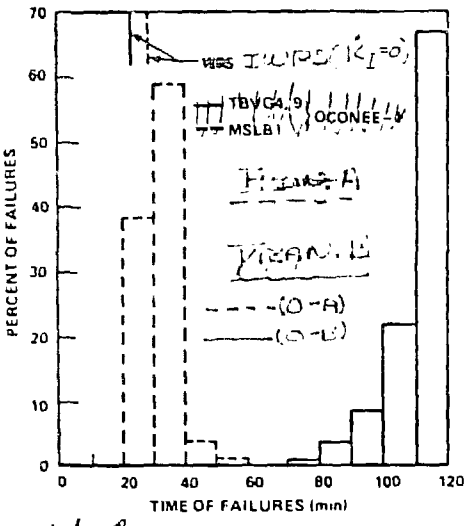

This is histogram of accident failures vs time of failure for three transients

ORNL WS-35623 ETD

WPS ($\dot{K}_I = 0$) APPLIED TO DOMINANT TRANSIENTS MAY REDUCE P(F|E) AND Φ(F) SIGNIFICANTLY

TRANSIENT (IN ORDER OF DOMINANCE)	PLANT		
	OCONEE-1	CC-1	HBR-HYPO
	$P(F\|E)_{WPS}/P(F\|E)$		
1	$<10^{-3}$	$<2 \times 10^{-3}$	9×10^{-3}
2	3×10^{-1}	1	$<2 \times 10^{-3}$
3	$<10^{-3}$	$<1 \times 10^{-2}$	$<2 \times 10^{-3}$
4	$<10^{-3}$	1×10^{-1}	$<2 \times 10^{-3}$
5	3×10^{-1}	$<5 \times 10^{-1}$	5×10^{-2}
	$\Phi(F)_{WPS}/\Phi(F)$		
	1×10^{-1}	2×10^{-1}	7×10^{-3}

Table of results for three plants